

Amino-nanopolystyrene exposures of oyster (*Crassostrea gigas*) embryos induced no apparent intergenerational effects

Tallec Kevin ^{1,*}, Paul-Pont Ika ⁴, Petton Bruno ¹, Alunno Bruscia Marianne ¹, Bourdon C ⁵, Bernardini Ilaria ^{2,3}, Boulais Myrina ¹, Lambert Christophe ⁴, Quere Claudie ¹, Bideau Antoine ⁵, Le Goic Nelly ⁴, Cassone Anne-Laure ⁵, Le Grand Fabienne ⁴, Fabioux Caroline ⁵, Soudant Philippe ⁴, Huvet Arnaud ^{1,*}

¹ Univ Brest, Ifremer, CNRS, IRD, LEMAR, 29280, Plouzane, France

² Dipartimento di Biomedicina Comparata e Alimentazione, Università degli Studi di Padova, Padova, 7 Italy

³ Department of Physical, Earth and Environmental Sciences, University of Siena, Via Mattioli 4, 53100 9 Siena, Italy.

⁴ Univ Brest, Ifremer, CNRS, IRD, LEMAR, 29280, Plouzane, France

⁵ Univ Brest, Ifremer, CNRS, IRD, LEMAR, 29280, Plouzane, France

* Corresponding authors : Kevin Tallec, email address : kevintallec2@gmail.com ; Arnaud Huvet, email address : arnaud.huvet@ifremer.fr

Abstract :

Early life stages (ELS) of numerous marine invertebrates must cope with man-made contaminants, including plastic debris, during their pelagic phase. Among the diversity of plastic particles, nano-sized debris, known as nanoplastics, can induce effects with severe outcomes in ELS of various biological models, including the Pacific oyster *Crassostrea gigas*. Here, we investigated the effects of a sub-lethal dose (0.1 µg mL⁻¹) of 50 nm polystyrene nanobeads (nano-PS) with amine functions on oyster embryos (24 h exposure) and we assessed consequences on larval and adult performances over two generations of oysters. Only a few effects were observed. Lipid analyses revealed that first-generation (G1) embryos exposed to nano-PS displayed a relative increase in cardiolipin content (+9.7%), suggesting a potential modification of mitochondrial functioning. G1-larvae issued from exposed embryos showed decreases in larval growth (-9%) and lipid storage (-20%). No effect was observed at the G1 adult stage in terms of growth, ecophysiological parameters (clearance and respiration rates, absorption efficiency), or reproductive outputs (gonadic development, gamete quality). Second generation (G2) larvae issued from control G1 displayed a significant growth reduction after G2 embryonic exposure to nano-PS (-24%) compared to control (as observed at the first generation), while no intergenerational effect was detected on G2 larvae issued from G1 exposed embryos. Overall, the present experimental study suggests a low incidence of a short embryonic exposure to nano-PS on oyster phenotypes along the entire life cycle until the next larval generation.

Keywords : Oyster, nanoplastics, embryonic exposure, larval performances, offspring

1) Introduction

Since 1950, mankind has produced 6,300 million tons (Mt) of plastic waste and a large part (~79%) was buried in landfills or dumped in the natural environment (Geyer *et al.*, 2017). Plastics debris are pervasive and contaminate all ecosystems including the marine environment as ultimate recipient (*e.g.* Cole *et al.*, 2011). Plastics debris are found everywhere in the oceans (*e.g.* sea ice, sediment, deep-sea) and it is estimated that 93–236,000 metric tons are presently floating on the surface of the open ocean (*e.g.* Paul-Pont *et al.*, 2018; van Sebille *et al.*, 2015). The largest proportion of oceanic plastic waste, in terms of the number of pieces, has been suggested to consist of microplastics (MP; < 5 mm) (*i.e.* 92% of plastic items at the open ocean sea surface; Eriksen *et al.*, 2014). These include manufactured particles (*e.g.* facial scrubs or exfoliants; primary MP) and particles derived from the fragmentation of larger debris in seawater (secondary MP) (Cole *et al.*, 2011). Fragmentation processes can lead to the creation of nano-sized debris, known as nanoplastics (NP <1 μm), as demonstrated under laboratory conditions (Gigault *et al.*, 2016; Lambert and Wagner, 2016; Dawson *et al.*, 2018; Ekvall *et al.*, 2018; Mateos-Cárdenas *et al.*, 2020) and recently underlined by the detection for the first time of plastic particles <1 μm in the North Atlantic subtropical gyre (Ter Halle *et al.*, 2017). In addition to the fragmentation processes, recent works detected primary NP in cosmetics (Hernandez *et al.*, 2017) or waste of industrial processes (Stephens *et al.*, 2013; Zhang *et al.*, 2012), being therefore possible direct sources in environment. Although environmental NP concentrations are still unknown and require new and adapted methods (Mintenig *et al.*, 2018), it is expected that their number concentrations exceed MP concentrations (Wagner and Reemtsma, 2019).

The potential impacts of micro- and nanoplastics (MNP) are recognized as a major concern (*e.g.* Galloway *et al.*, 2017). Overall, the first insights revealed that NP can induce a higher toxicity than MP due to nano-properties, *i.e.* their nano-size and high surface-to-volume ratio enhance their reactivity and interactions with biological membranes and, therefore the risk of damages and/or particle translocations into tissues/organs (Al-Sid-Cheikh *et al.*, 2018; Jeong *et al.*, 2016; Paul-Pont *et al.*, 2018). Various kinds of damage have been recorded in aquatic organisms upon laboratory exposures to NP, *e.g.* decrease in reproduction and/or growth (Jeong *et al.*, 2016; Besseling *et al.*, 2014), behavior modifications (Chen *et al.*, 2017), energy balance disruptions (Trevisan *et al.*, 2019), immune perturbations (Auguste *et al.*, 2020), alteration of cell homeostasis by membrane injury/modifications (Feng *et al.*, 2019). Most effects have been demonstrated at the individual level, but recent findings suggested transgenerational effects

(Zhao *et al.*, 2017; Liu *et al.*, 2020). For instance, 2-generations exposure to nanopolystyrene beads ($1 \mu\text{g}\cdot\text{L}^{-1}$) reduced growth and reproduction in the recovery generation of daphnia (Liu *et al.*, 2020). To investigate toxic potential of nanoplastics, commercial nanopolystyrene beads are used, notably amino-nanopolystyrene beads ($-\text{NH}_2$) due to their properties: (i) no aggregation in experimental seawater and (ii) a positive charge promoting interactions with biological membranes (*e.g.* Della Torre *et al.*, 2014; Lehner *et al.*, 2019).

Many marine invertebrates are characterized by external fertilization followed by a free larval development in seawater (Pechenik, 1999). Thus, early life stages (ELS) must cope with stressors in seawater, notably in coastal areas that are heavily affected by human activities (Halpern *et al.*, 2008). ELS are commonly used as biological models in risk assessments notably to evaluate the toxicity of plastic debris (*e.g.* Beiras *et al.*, 2018). In this regard, first reports indicated a high sensitivity of ELS to NP, in particular during the embryogenesis (Balbi *et al.*, 2017; Della Torre *et al.*, 2014; Tallec *et al.*, 2018). Embryogenesis is a key step characterized by intense morphological, cellular and molecular changes that make embryos highly sensitive to external disruptors (Fitzpatrick *et al.*, 2008; Sokolova *et al.*, 2012; Bhandari *et al.*, 2015). In most cases, embryos harbor the genetic information carried over successive generations through germline differentiation during the first cleavages of embryogenesis (Leclère *et al.*, 2012). Therefore, modifications of embryogenesis can lead to effects over generations (Bhandari *et al.*, 2015; Major *et al.*, 2020) but no data is available, to our knowledge, on the potential repercussions of embryonic exposure to NP on subsequent stages (*e.g.* larvae, adults) and next generations. The present study aims to address this question by using the Pacific oyster (*Crassostrea gigas*) which is a key species in coastal systems. Early life stages of *C. gigas* are commonly used as marine biological model (*e.g.* Mottier *et al.*, 2013; Sussarellu *et al.*, 2018). As demonstrated previously using a standardized bivalve embryotoxicity assay (AFNOR XP-T-90-382), oyster embryos are sensitive to 50-nm nanopolystyrene beads, especially those with an amine functionalization (50- NH_2) with an EC_{50} of $0.15 \mu\text{g}\cdot\text{mL}^{-1}$ (Tallec *et al.*, 2018). Overall, oyster embryos displayed similar sensitivity than mussel embryos (50- NH_2 exposure, EC_{50} : $0.14 \mu\text{g}\cdot\text{mL}^{-1}$; Balbi *et al.*, 2017) but higher than other ELS models such as sea urchins embryos (50- NH_2 exposure, EC_{50} : $2.61 \mu\text{g}\cdot\text{mL}^{-1}$; Della Torre *et al.*, 2014), rotifer larvae (50- NH_2 exposure, EC_{50} : $2.75\text{--}6.62 \mu\text{g}\cdot\text{mL}^{-1}$, Manfra *et al.*, 2017) or zebrafish embryos (20 nm PS beads exposure, EC_{50} : $21.5\text{--}52.2 \mu\text{g}\cdot\text{mL}^{-1}$; Zhang and Goss, 2020). With the aim of testing the consequences of sub-lethal effects induced by these particles on embryonic development, including potential effects at the adult stage and imprinting affecting the next generation, the

present study assessed effects of short term (24h) embryonic exposure to 50-NH₂ beads at a sub-lethal dose (0.1 µg.mL⁻¹; Tallec *et al.*, 2018) over two generations. Effects on oyster performances were examined at both larval (growth, development, settlement) and adult stages (growth, clearance and respiration rates, reproductive outputs) at the first generation and on larval performances at the second generation.

2) Materials and methods

2.1) Nanopolystyrene beads

Nanopolystyrene beads (nano-PS; 50 nm) with an amine functionalization (50-NH₂) were purchased from Bangs Laboratories (USA). This nano-PS did not have any fluorescent labelling. Polystyrene polymer chemistry was confirmed by Raman microspectroscopy (LabRAM HR800 Raman; Horiba Scientific; Japan) (Tallec *et al.*, 2018). Particles were characterized in 1-µm filtered, UV-treated seawater (SW; 20°C, pH 8.1, PSU 34, I 0.678 mol.L⁻¹) by Dynamic Light Scattering (DLS; Zetasizer NanoZS; Malvern Instruments; UK) at a concentration of 100 µg.mL⁻¹. This concentration was used for DLS analysis owing to the occurrence of artifacts at lower concentrations. DLS results showed that the 50-NH₂ suspension formed at T₀ and T_{24h} small aggregates (97 ± 2 nm) in SW with a positive surface charge (16 ± 3 mV) (see details in Tallec *et al.*, 2018). The stock suspension was kept at 4°C and diluted in ultrapure water at 1 mg.mL⁻¹ just before the final dilution in SW for the exposures.

2.2) Broodstock

The initial broodstock (18-month-old-mature oysters *C. gigas*; generation 0, G0) was collected from a farming area in the Bay of Brest (48°20'6''N, 4°19'6''W; seawater features: 18.9°C, pH 8.0, PSU 34.6) before being transferred to Ifremer's experimental facilities (Argenton, France) in June 2018. These oysters were acclimatized in a 350 L tank supplied with SW (16.5°C) containing a balanced mixture of two microalgae, *Tisochrysis lutea* (T-iso CCAP927/14, cell volume = 40 µm³) and *Chaetoceros* sp. (CCAP 1010/3, cell volume = 80 µm³).

2.3) Experimental design

The experimental design used to breed, expose and rear oysters over two generations is summarized in Figure 1. The first generation of oyster embryos (G1) was produced in June 2018 from the initial broodstock G0 according to a standardized bivalve embryotoxicity assay (AFNOR XP-T-90-382) adapted to an aquaculture experimental design. Gametes from 5 males and 5 females were collected by stripping. Precautions were taken to avoid polyspermy: oocytes

were incubated in SW during 45 minutes before fertilization and the spermatozoa-to-oocyte ratio was set at a much lower ratio than the one identified as leading to high risk of polyspermy in oysters (1000:1; Bayne, 2017; Alliegro and Wright, 1983, Stephano and Gould, 1988). Gametes were pooled in 1.8 L of SW (21°C) with a spermatozoa-to-oocyte ratio of 100:1 and a final concentration of 1,000 oocytes.mL⁻¹. Gamete concentrations were estimated using an EasyCyte Plus cytometer (Guava Merck Millipore, USA). The fertilization yield (%; [number of fertilized oocytes/number of oocytes] × 100) estimated after 1.5 h of contact between gametes was 95 ± 3% (n = 12 beaker replicates). Thereafter, G1 embryos (2-4 cells) were placed in 5-L glass beakers (100 embryos.mL⁻¹; 21°C) and divided into two treatments (n = 12 beaker replicates per treatment; Step 1): G1 embryos without exposure corresponding to the control (G1-C) and G1 embryos exposed to 50-NH₂ beads at 0.1 µg.mL⁻¹ (G1-E). The embryonic exposure lasted 24 h, which corresponds to the time needed to reach the final stage of oyster embryogenesis, the D-larva (Robert & Gerard, 1999). Therefore, all the embryonic stages, 2-4-8 cells, morula, blastula, gastrula, and trochophore were exposed. At the end of the exposure, all beaker contents were sieved at 40 µm to estimate the D-larval yield (%; number of D-larvae / number of fertilized oocytes × 100) and the normal D-larval yield (%; number of normal D-Larvae / (number of normal D-Larvae + number of abnormal D-Larvae) × 100). Abnormal D-larvae referred to mantle and/or shell malformations or developmental arrest during embryogenesis (Mottier *et al.*, 2013). Lipid (see section 2.4) and scanning electron microscopy (see section 2.5) samplings were also performed at this step. The remaining normal D-larvae were rinsed with SW to remove the nano-PS and 100,000 individuals per replicate and per treatment were transferred to the larval rearing system to complete their pelagic phase until settlement (≈ 16 days post fertilization, dpf) in order to evaluate mid-term consequences (larval performances) of the embryonic exposure (see section 2.6; Step 2). All nano-PS contaminated waters were stored in sealed containers and treated as hazardous chemicals.

Long-term consequences of the embryonic exposure were investigated on adult performances (G1) and larval performances of the next generation (G2). Once larvae settled, 2,000 G1 oyster seeds per treatment (G1-C and G1-E; 50 days old) were transferred to the Ifremer nursery (Bouin, France) in August 2018, where they were reared in onshore facilities for 8 months with UV-treated, filtered seawater and *Skeletonema costatum ad libitum*. Oyster growth was monitored every 1–2 months over this period (see section 2.7). In April 2019, 632 adult oysters per treatment (G1-C and G1-E; 10 months old) were returned to Ifremer's experimental facilities in Argenton to complete gametogenesis. These oysters were placed in four 350-L tanks

in a common garden scheme (158 oysters per treatment per tank) in order to avoid any bias due to putative differences among the four tanks and their positions in the experimental room. G1 adult oysters were maintained for 10 weeks at 17°C and fed continuously on a mixed diet of *T. lutea/Chaetoceros* sp. (50/50, v/v) at a mean concentration of 2,000 $\mu\text{m}^3 \cdot \mu\text{L}^{-1}$ to ensure complete gametogenesis (conditioning period). Oyster growth and ecophysiology (clearance and respiration rates, absorption efficiency) were monitored throughout this conditioning period (see section 2.8; Step 3).

After 10 weeks of conditioning, once the G1 oysters were mature, the sex ratio and gamete quality were compared between treatments (G1-C and G1-E; see section 2.9). The second generation of embryos (G2) was produced by pooling oyster gametes within each treatment following the same protocol described above (Step 4). There were four treatments in the G2 embryonic exposure experiment (n = 4 beaker replicates per treatment; n was reduced as number of treatment has increased in comparison to the G1 experiment): (i) G2 embryos from G1-C adults with no G2 embryonic exposure (G2-C-C), (ii) G2 embryos from G1-C adults with G2 embryonic exposure to 50-NH₂ beads at 0.1 $\mu\text{g} \cdot \text{mL}^{-1}$ (G2-C-E), (iii) G2 embryos from G1-E adults without G2 embryonic exposure (G2-E-C), (iv) G2 embryos from G1-E adults with G2 embryonic exposure to 50-NH₂ beads at 0.1 $\mu\text{g} \cdot \text{mL}^{-1}$ (G2-E-E). As in the G1, embryonic exposure was stopped after 24h, the D-larval and normal D-larval yields were estimated then 100,000 normal D-larvae per replicate per treatment were rinsed and placed in the larval rearing system to complete the pelagic phase.

[Figure 1 near here]

2.4) Lipid composition (G1 – Step 1)

Potential lipid content (classes and fatty acids) modifications were investigated because membrane impairments are proposed as leading cause of the nano-PS toxicity (*e.g.* Feng *et al.*, 2019; González-Fernández *et al.*, 2020). At the end of the G1 embryonic development and nano-PS exposure, 200,000 normal D-larvae per replicate per treatment were collected on GF/F glass-fibre filters (0.2 μm ; Whatman[®]; burnt beforehand at 450°C for 6 h). Their lipid content was extracted in 6 mL chloroform:methanol (2:1 v/v) and stored at -20°C (Da Costa *et al.*, 2016). Lipid class composition was determined by high-performance thin layer chromatography (HPTLC) using glass plates coated with silica (200×100 mm; Merck[®]60, Germany) (Da Costa *et al.*, 2016). To specifically analyse neutral lipids (NL) and polar lipids (PL), plate preparations were conducted using different mixtures: (i) hexane:diethyl ether (97:3;

v/v) for NL; (ii) methyl acetate:isopropanol:chloroform:methanol:0.25% KCl (10:10:10:4:3.6; v/v) for PL. Thereafter, lipid extracts were spotted onto these plates using an automatic TLC sampler ATS4 (CAMAG[®]; Switzerland). Separation of NL was performed using two successive mixtures: (1) hexane:diethyl ether:acetic acid (20:5:0.5; v/v); (2) hexane:diethyl ether (97:3; v/v). Separation of PL was made with a mixture of methyl acetate:isopropanol:chloroform:methanol:0.25% KCl (10:10:10:4:3.6; v/v). Plates were revealed using a 3% CuSO₄ and 8% H₃PO₄ (w/v in distilled water) solution, then analysed with a scanner densitometer at 370 nm (TLC Scanner 4 CAMAG[®]; Switzerland). Results were analysed using VisionCATS software (v2.5; CAMAG[®]; Switzerland) (Moutel *et al.*, 2016). Lipid classes were expressed as the mass percentage of each class in the total lipid content of a D-larva (ng.D-larva⁻¹). Analyses of NL and PL allowed identification of: (i) three classes of storage lipids: triglycerides (TG), sterol esters (StE) and glyceryl ethers (GE); (ii) one class used as a proxy of lipid degradation: free fatty acids (FFA); (iii) seven classes of membrane lipids: phosphatidylethanolamine (PE), phosphatidylinositol (PI) + ceramide aminoethylphosphonate (CAEP), phosphatidylserine (PSer), cardiolipin (CL), phosphatidylcholine (PC) and sterols (ST).

To examine fatty acid (FA) composition, 1 mL of lipid extract was evaporated under N_{2(g)}, recovered by three chloroform:methanol (98:2, v/v) washings (0.5 mL), then deposited at the top of a silica micro-column (40 × 5 mm) to separate the polar and neutral fractions as described in Le Grand *et al.* (2014). Samples were successively evaporated under N_{2(g)} and transesterified in 800 µL MeOH-H₂SO₄ (3.4% v/v) for 10 min at 100 °C to obtain fatty acid methyl esters (FAME). FAME were analysed using a Varian CP8400 gas chromatograph (HP, USA) according to Le Grand *et al.* (2014). FAs were expressed as the mass percentage of each FA in the total FA content per fraction (neutral or polar).

2.5) Scanning electron microscopy (G1 – Step 1)

Aliquots of G1-C and G1-E D-larvae were fixed for 1h in a mixture of 6% glutaraldehyde:7 % NaCl:0.4 M cacodylate (2:1:1; v/v) before being rinsed in a mixture of 0.4 M cacodylate:8% NaCl:ultrapure water (1:1:2; v/v; 3 baths, 15 min). Thereafter, samples were dehydrated in the following successive solutions: (1) 50% ethanol (2 baths, 10 min); (2) 70% ethanol (2 baths, 10 min); (3) 90% ethanol (2 baths, 10 min); (4) absolute ethanol (3 baths, 15 min); (5) absolute ethanol:hexamethyldisilazan (HMDS) (3:1, v/v; 15 min); (6) absolute ethanol:HMDS (1:1, v/v; 15 min); (7) absolute ethanol:HMDS (1:3, v/v; 15 min); (8) pure HMDS (2 baths, 15 min) according to Foulon *et al.* (2016). Lastly, samples were coated with gold palladium and

scanning electron microscopy (SEM) observations (Hitachi S-3200N, Japan) were performed on a dozen of larvae per treatment. G2 D-larvae could unfortunately not be analysed due to a failed fixation of larvae.

2.6) Larval rearing and settlement (G1 – Step 2 and G2 – Step 5)

G1 and G2 larvae were reared in 5-L cylinders at a density of 20 larvae.mL⁻¹ using a flow-through rearing system at 25°C (Rico-Villa *et al.*, 2008). Cylinder replicates (12 per treatment for G1 and 4 per treatment for G2) were randomly positioned in the system. Larvae were continuously supplied with SW containing a mixed diet of *T. lutea*/*C. neogracile* (50/50, v/v) at a mean concentration of 1,500 µm³.µL⁻¹. For G1 and G2, aliquots of 20 to 30 larvae were sampled every 2–3 days from each cylinder and fixed in a formaldehyde-seawater solution (0.1% final) to evaluate the larval growth by image analysis using ImageJ software. For G1, when more than 50% of larvae reached the metamorphosis-competent stage (*i.e.* eyed-larvae stage) in each replicate per treatment, the treatment was sieved on 80-µm mesh and 20,000 larvae were transferred to 30-L tanks at 25°C to settle on cultch using a downwelling system (n = 4–6 batches per treatment for G1 and n = 2 for G2) as described in Petton *et al.* (2013). For G2, another method was used, all treatments were settled in the same time, when more than 50% of larvae in one treatment had reached the metamorphosis-competent stage. As settlement measurements were not performed following the same protocol, results for this endpoint were therefore not comparable between generations. For G1 and G2 an aliquot of competent eyed-larvae (n = 10 larvae per replicate) was sampled and stained with a SW-Nile Red (0.00125 mg.mL⁻¹) solution for 1.5 h before fixation in a formaldehyde-seawater solution (0.1% final) to evaluate the lipid index (arbitrary units, A.U.), *i.e.* the relative amount of storage lipids, using a Zeiss AxioObserver Z1 (Germany). The lipid index for one larva was defined as: fluorescent area/total area (Talmage and Gobler, 2010). Image analysis was again performed using ImageJ software. In the settlement system, larvae were fed continuously on the same diet used for the larval rearing. After 14 days in the downwelling system, all tanks were sieved on 400-µm mesh to evaluate the settlement yield (%) defined as: (number of settled larvae/number of total larvae) × 100. The G1 settled larvae were again put in the downwelling system before being transferred to the Ifremer nursery (Bouin, France) for the growth period (August 2018 – March 2019).

2.7) Adult growth monitoring (G1 – Step 3)

G1 adult growth was monitored at the Ifremer nursery by sampling 30 oysters per treatment in November 2018, January, February and March 2019. The collected oysters were stored at -20°C until measurements of the dry flesh mass used as a proxy of oyster growth (Savina and

Pouvreau, 2004). Similarly, 20 oysters per treatment per tank were sampled for growth measurements at 3, 5, 7 and 10 weeks after the beginning of the conditioning period in Argenton (April–June 2019).

2.8) Ecophysiological measurements (G1 – Step 3)

An ecophysiological measurement system was used to determine the individual clearance (CR; $L \cdot h^{-1} \cdot ind^{-1}$) and respiration (RR; $mg \ O_2 \cdot h^{-1} \cdot ind^{-1}$) rates of G1 adult oysters (G1-C and G1-E). This system consists of nine individual flow-through chambers (0.54 L) supplied with seawater pumped into the conditioning tank at a constant flow rate of $30 \ mL \cdot min^{-1}$. These chambers are managed by a programmable controller that enables high-frequency automatic recordings of fluorescence (food supply), oxygen concentrations, and water flow in the seawater outflow (Pousse *et al.*, 2018). We used a WTW multiparameter meter (WTW Multi 3430), a WETStar fluorimeter (WSCHL-1400 WETLABS; USA) and a SONOFLOW CO.55 ultrasonic flow rate meter (Sonotec; Germany). For each set of measurements (also referred to here as trials), all the biological and physico-chemical parameters mentioned above were recorded every 3.5 h over 4 days on four oysters per treatment, with each of the oysters in a separate individual chamber. This procedure was replicated four times, thus collecting individual data from 16 oysters per treatment by the end of the adult experiment. For each trial, one chamber was left empty, thus providing a control chamber (CC). The individual clearance rate (CR) of each oyster is estimated as: $CR = (fl \times (C_{CC} - C_N) / C_{CC})$, where fl is the flow rate through the chamber ($L \cdot h^{-1}$), C_{CC} is the concentration of microalgae in the control chamber and C_N is the concentration of microalgae in a chamber with one oyster (Bayne, 2017). The individual respiration rate is defined as: $RR = fl \times (O_{CC} - O_N)$, where fl is the flow rate through the chamber ($L \cdot h^{-1}$), O_{CC} and O_N are the concentrations of O_2 ($mg \ O_2 \cdot L^{-1}$) in the control chamber and in a chamber with one oyster, respectively (Savina and Pouvreau, 2004). At the end of each trial, all oysters were sacrificed and stored at $-20^\circ C$ before measuring the dry flesh mass in order to calculate mass standardized clearance and respiration rates for an equivalent individual of 1 g dry tissue (dw std) (Bayne *et al.*, 1987). In addition, absorption efficiency (AE, %) of organic matter from ingested microalgae was calculated according to Conover's method by collecting faeces twice a week from each chamber: $AE = (f - e) / ((1 - e) \times f)$, where f corresponds to the organic fraction of the diet and e is the organic fraction of the faeces (Conover, 1966).

2.9) Reproductive measurements (G1 – Step 3)

The gonadic development and sex ratio were assessed by histology on 20 oysters per treatment every 2 weeks during the conditioning period. A 3 mm cross-section of the visceral mass was

cut and fixed in modified Davidson's solution at 4°C for 48h. Thereafter, samples were dehydrated in ascending ethanol solutions, embedded in wax paraffin and stained with Harris' hematoxylin-eosin as described in Fabioux *et al.*, (2005). Sections were observed under a microscope (Leica DMIRB; Germany) and gametogenic stages determined according to Steele and Mulcahy (1999).

Once the G1 oysters were reproductively mature, four pools of spermatozoa and oocytes, each issued from 5 males and 5 females, respectively (total number = 40 oysters per treatment), were used to examine gamete quality and fertilization efficiency. Spermatozoa behavior (percentage of motile spermatozoa and Velocity of the Average Path (VAP; $\mu\text{m}\cdot\text{sec}^{-1}$) were analysed using a CASA (computer-assisted sperm analyser) plug-in for ImageJ according to Boulais *et al.* (2015); a minimum of 100 spermatozoa per replicate were analysed. Briefly, 100 μL of the spermatozoa solution (1×10^8 spermatozoa. mL^{-1}) of each replicate were diluted in 300 μL of SW containing pluronic acid ($1 \text{ g}\cdot\text{L}^{-1}$), then placed in FastRead cells (Fischer Scientific®, USA) to acquire videos (Camera Qicam Fast 1394, 60 frames. sec^{-1} , 6 sec.treatment $^{-1}$) under a microscope (Olympus BX51, Japan; $\times 20$ magnification, dark field) (Boulais *et al.*, 2015). For oocytes, aliquots were fixed in a formaldehyde-seawater solution (0.1% final) and oocyte pictures were taken under a microscope (Olympus BX51, Japan; $\times 10$ magnification). Oocyte diameter (μm) was assessed using ImageJ (30 oocytes were measured per replicate) as in Sussarellu *et al.* (2016). Gametes from the same treatment were mixed using the method described in section 2.3 (spermatozoa-to-oocyte ratio of 100:1 and 1,000 oocytes. mL^{-1} ; final volume: 1.8 L; n = 4 beaker replicates per treatment) to estimate the fertilization yield (used as a proxy of the reproductive capacity) after 1.5 h of contact.

2.10) Statistical analyses

All statistical analyses and graphical representations were done using R software (R Core Team, 2016). Normality and variance homogeneity were verified using Shapiro-Wilk and Levene's methods, respectively. To compare fertilization yield (G2: 4 \times 10 oysters [5 males + 5 females] per treatment), D-larval yield (G1: 12 batches of 500,000 embryos; G2: 4 batches of 500,000 embryos), lipid index (G1: 12 \times 10 larvae per treatment; G2: 4 \times 10 larvae per treatment), survival (G1: 12 batches of 100,000 larvae per treatment; G2: 4 batches of 100,000 larvae per treatment), settlement yield (G1: 4-6 batches of 20,000 per treatment), absorption efficiency (G1: 16 oysters per treatment), and gamete quality (G1: 4 \times 10 oysters [5 males + 5 females] per treatment), the Student's tests or one-way ANOVA were performed according to the number of treatments. Percentages were analysed after angular transformations. Repeated

measures ANOVA were conducted on growth (adults and larvae) and ecophysiological measurements (G1: 16 oysters per treatment) with pairwise comparisons using Tukey's method when necessary. Comparisons among lipid class proportions (G1: 12 batches of 100,000 larvae per treatment) were made using Student's method while comparisons between fatty acid compositions (G1: 12 batches of 100,000 larvae per treatment) were screened using one-way analyses of similarities (ANOSIM) and a Bray-Curtis similarity matrix to separate clusters ($R = 1$: perfect separation; $R = 0.5$: satisfactory separation, $R = 0$: low separation cluster). Fisher tests were used to compare sex ratio and gonadic development between treatments (20 oysters per treatment). Data were expressed as the mean \pm standard error (SE) and differences were considered significant when p-values < 0.05 .

3) Results

3.1) *Effects of embryonic exposure to nano-PS on the first oyster generation (G1)*

3.1.1) *D-larval yield (Step 1)*

At the end of embryonic development (24 hours post fertilization, hpf), D-larval yields were similar in the control (G1-C; $73.9 \pm 1.8\%$) and exposed treatments (G1-E; $74.3 \pm 2.3\%$). No differences in the abnormality level were detected between treatments under optical microscopy (average normal D-larval yield = $87.7 \pm 0.6\%$). Scanning electron microscopy (SEM) observations revealed holes and/or surface asperities on 9 of the 12 observed G1-E D-larvae (75%) while these were only observed in 3 of the 12 observed G1-C D-larvae (3) (Figure 2).

[Figure 2 near here]

3.1.2) *Lipid composition of D-larvae (Step 1)*

Lipid classes. D-larvae from the different treatments had a similar total mass of lipids (9.2 ± 0.1 and 9.5 ± 0.3 ng.D-larva⁻¹ for G1-C and G1-E, respectively; p-value > 0.05) and no significant differences were observed in the percentages of storage and membrane lipids between the G1-E D-larvae ($55.3 \pm 0.7\%$ and $44.7 \pm 0.7\%$, respectively) and the G1-C D-larvae ($55.4 \pm 0.5\%$ and $44.7 \pm 0.5\%$, respectively). In terms of lipid class composition, only the relative percentage of cardiolipin (CL) was statistically different between treatments, being 9.7% higher (p-value < 0.01) in G1-E D-larvae compared with G1-C D-larvae (Table 1).

Fatty acid (FA) composition. The FA composition of the G1-E D-larvae was similar to that of the G1-C D-larvae according to the one-way ANOSIM ($R = 0.109$ and $R = -0.031$ for polar and neutral fractions, respectively; p-values > 0.05 ; Supplementary Tables 1 and 2).

[Table 1 near here]

3.1.3) Larval performances: growth, lipid index and settlement yield (Step 2)

G1 larvae from the G1-E treatment had a significantly lower growth rate (GR) than control larvae (G1-C; p -value < 0.05 ; Figure 3A). The GR was 8.7% lower in G1-E larvae ($17.8 \pm 0.5 \mu\text{m}\cdot\text{day}^{-1}$) compared with G1-C larvae ($19.5 \pm 0.4 \mu\text{m}\cdot\text{day}^{-1}$). Consequently, the G1-E larvae displayed a delay of one day to reach the competent larval stage, as shown by the percentages of eyed-larvae (ready to settle) at 16 dpf: $55.5 \pm 3.3\%$ for G1-C and $24.8 \pm 2.6\%$ for G1-E larvae. The survival was similar (p -value > 0.05) between treatments (Supplementary Table 3). The lipid index (A.U.) differed significantly between treatments with a mean reduction of 19.6% in G1-E larvae compared with G1-C larvae (p -value < 0.01 ; Figure 3B). The settlement yield (%) was statistically similar between G1-C and G1-E treatments (p -value > 0.05 ; Figure 3C).

[Figure 3 near here]

3.1.4) Adult growth and ecophysiological performances (Step 3)

Growth. The monitoring of G1 juvenile and adult growth revealed no statistical differences whether they originated from control or exposed embryos (p -value > 0.05 ; Figure 4). Data collected in the nursery (November 2018 – March 2019) showed that the dry mass of tissues increased 3-fold in both G1-C (T_{November} : $0.06 \pm 0.01 \text{ g}\cdot\text{oyster}^{-1}$; T_{March} : $0.16 \pm 0.01 \text{ g}\cdot\text{oyster}^{-1}$) and G1-E oysters (T_{November} : $0.05 \pm 0.01 \text{ g}\cdot\text{oyster}^{-1}$; T_{March} : $0.17 \pm 0.01 \text{ g}\cdot\text{oyster}^{-1}$). Similarly, during the conditioning period, the dry mass of tissues was $0.15 \pm 0.01 \text{ g}\cdot\text{oyster}^{-1}$ for G1-C and G1-E oysters at T_0 (April 2019) and increased up to 0.48 ± 0.03 and $0.53 \pm 0.04 \text{ g}\cdot\text{oyster}^{-1}$ for G1-C and G1-E oysters, respectively, by T_f (June 2019), corresponding to a 3-fold increase in both treatments.

[Figure 4 near here]

Ecophysiological parameters. No significant differences (p -values > 0.05) were observed in individual clearance rate (CR; $\text{L}\cdot\text{h}^{-1}\cdot\text{g}^{-1} \text{ dw std}$), respiration rate (RR; $\text{mg O}_2\cdot\text{h}^{-1}\cdot\text{g}^{-1} \text{ dw std}$) or absorption efficiency (AE; %) between adult oysters of both treatments throughout the experiment (Figure 5; Supplementary Figure 1).

[Figure 5 near here]

3.1.5) *Reproductive outputs (Step 3)*

Overall, adult oysters issued from the two treatments showed similar sex ratios and distributions of gonadic stages (p-values > 0.05), resulting in 85% and 95% of mature oysters after 10 weeks of conditioning for G1-C and G1-E treatments, respectively (Table 2; Supplementary Figure 2).

Regarding gamete quality, percentages of motile spermatozoa (%) were similar (p-values > 0.05) between G1-C ($41.8 \pm 1.6\%$) and G1-E oysters ($43.6 \pm 3.0\%$) as were the mean velocities (VAP; $\mu\text{m}\cdot\text{sec}^{-1}$), estimated at $72.1 \pm 1.1 \mu\text{m}\cdot\text{sec}^{-1}$ and $79.8 \pm 4.4 \mu\text{m}\cdot\text{sec}^{-1}$, respectively. Similarly, oocyte diameters (μm) were identical (p-value > 0.05) between G1-C ($30.5 \pm 0.2 \mu\text{m}$) and G1-E oysters ($30.7 \pm 0.4 \mu\text{m}$). Lastly, the reproductive success was not affected by treatment, as demonstrated by high and similar fertilization yields (%) of $90.5 \pm 1.2\%$ for G1-C oysters and $87.3 \pm 2.3\%$ for G1-E oysters.

[Table 2 near here]

3.2) *Effects of embryonic exposure to nano-PS on the second oyster generation (G2)*

3.2.1) *D-larval yield (Step 4)*

No significant differences were observed in D-larval yields among the four treatments (p-value > 0.05) with mean values of $67.1 \pm 4.8\%$, $60.4 \pm 3.5\%$, $64.4 \pm 5.1\%$ and $59.5 \pm 8.1\%$ for G2-C-C, G2-E-C, G2-C-E and G2-E-E, respectively. No differences in the abnormality level were detected between treatments under optical microscopy (average normal D-larval yield = $80.5 \pm 2.8\%$).

3.2.2) *Larval performances: growth, lipid index and settlement yield (Step 5)*

The G2 larval growth fell into two statistical groups (p-value < 0.05; Figure 6A). G2-C-C and G2-E-C larvae had similar growth rates (p-value > 0.05) with mean values of $17.1 \pm 0.7 \mu\text{m}\cdot\text{day}^{-1}$ and $16.9 \pm 0.3 \mu\text{m}\cdot\text{day}^{-1}$, respectively. G2-C-E larvae ($12.9 \pm 1.8 \mu\text{m}\cdot\text{day}^{-1}$) had a significantly slower growth (-24%) than G2-C-C and G2-E-C larvae (p-value < 0.05), while G2-E-E larvae had an intermediate growth non-significantly different from any of the other groups (G2-C-C, G2-E-C and G2-C-E) with a mean growth rate of $14.5 \pm 2.5 \mu\text{m}\cdot\text{day}^{-1}$. At the end of the larval rearing (17 dpf), a delay to reach the competent larval stage was suggested with a lower percentage of eyed-larvae in the G2-C-E treatment ($20.0 \pm 8.2\%$) compared with G2-C-C ($49.0 \pm 4.5\%$), G2-E-C ($43.7 \pm 12.0\%$) and G2-E-E ($32.8 \pm 10.9\%$) larvae. Survival was similar (p-value > 0.05) among treatments (Supplementary Table 3). Conversely to G1 larvae, no significant differences (p-value > 0.05) in lipid index (A.U.) were observed among G2 larvae

treatments (Figure 6B). The settlement yield appeared similar (no statistical test was made as there were only two replicates per treatment) among G2 larvae treatments (Figure 6C).

[Figure 6 near here]

4) Discussion

Direct effects of nano-PS exposure during oyster embryonic development. Embryogenesis is a sensitive step in the life cycle of marine invertebrates. This sensitivity is linked to the balance between embryogenic trajectories governed by molecular/cellular programming and the surrounding conditions with its external pressures, notably stressors, for which embryos can show developmental plasticity (Hamdoun and Epel, 2007). Energy metabolism, *e.g.* glucose and lipid metabolism, is crucial for embryo development (*e.g.* Jaeckle and Manahan, 1989; Rafalsky *et al.*, 2012). Among lipids composition, cardiolipin (CL) appeared modified, with a greater relative proportion in D-larvae issued from exposed embryos (+9.7%). CL is a key and unique phospholipid located in the inner membrane of mitochondria, being the primary supplier of energy (ATP) used by organisms for basal maintenance, growth, development and storage (Houtkooper and Vaz, 2008; Sokolova *et al.*, 2012). Specifically, CL has a major role in the functioning of oxidative phosphorylation, allowing the formation of ATP from ADP as it binds to oxidative phosphorylation complexes to ensure their stability and ATP production (Houtkooper and Vaz, 2008; Paradies *et al.*, 2014). Therefore, the observed increase in the relative CL content may suggest modification in the respiratory chain in oyster embryos exposed to 50-NH₂ beads. For instance, an increase in CL proportion can affect cell bioenergetics, associated with a decrease in the membrane electron flux and in ATP synthesis (Julienne *et al.*, 2014; Shaikh *et al.*, 2014). In parallel, recent findings demonstrated that nano-PS beads can reduce ATP production; *e.g.* a decrease of 49–65% in ATP production by zebrafish embryos exposed to 50-nm PS-beads at 10 µg.mL⁻¹ (Trevisan *et al.*, 2019). Such impairment may alter the overall embryo energy balance at the expense of key maintenance and developmental processes, leading to a slower larval growth as observed here. As ATP production was not measured here, further investigations including transcriptomic analyses and biochemical assays of mitochondrial functioning at each step of embryo development, coupled with bioenergetic modelling, would help testing this hypothesis.

Regarding the ability of nano-PS to impact cell membranes (Rossi *et al.*, 2014; Feng *et al.*, 2019; González-Fernández *et al.*, 2020), lipid analyses showed no effect of 50-NH₂ at 0.1

$\mu\text{g.mL}^{-1}$ on external membranes composition and integrity of oyster embryos. Nevertheless, we cannot exclude that higher concentrations could lead to membrane disruptions, as suggested by the drastic developmental arrests previously observed in oyster embryos exposed to higher doses (from $1 \mu\text{g.mL}^{-1}$) of nano-PS beads (Tallec *et al.*, 2018). Such a loss of membrane integrity was, for example, highlighted in cyanobacteria exposed to 50-NH₂ beads at 2.5 and $4 \mu\text{g.mL}^{-1}$ (Feng *et al.*, 2019).

In agreement with high D-larval yield (>80%), malformations or developmental arrests were not observed by optical microscopy, indicating there was no strong acute toxicity upon exposure to nano-PS at $0.1 \mu\text{g.mL}^{-1}$ determined as sub-lethal. SEM observations revealed holes and asperities on the shells of D-larvae mostly issued from exposed embryos, however the low number of larvae analysed ($n = 12$) makes impossible to draw any firm conclusion. In previous literature, disruption of calcium carbonate production and deposition was suspected in mussel embryos after 50-NH₂ exposure ($0.15 \mu\text{g.mL}^{-1}$) based on transcriptomic profiles (Balbi *et al.*, 2017). Because shell of bivalve larvae have an essential protective role (against physical damage, pathogens, predators or pollutants; Arivalagan *et al.*, 2017), investigations of shell biomineralization in marine bivalves in response to nanoplastics exposure combining both – omics approach and high throughput SEM observations would be of relevant interest.

Repercussions of the embryonic exposure on oyster larval growth. Typically, in *C. gigas* the time to reach the competent stage in the used rearing system at 25°C is around 16 dpf as observed for the G1 and G2 larval rearing originated from unexposed embryos with size of competent larvae aligned with those from the literature ($\approx 300 \mu\text{m}$) (*e.g.* Rico-Villa *et al.*, 2008).

Many studies have examined the effects of contaminants on early life stages (ELS), but the consequences of sub-lethal effects in ELS performances later in life remain mostly undetermined despite their crucial role in species sustainability. The decrease in larval growth and the delay in reaching metamorphosis-competent stage observed in treatments exposed only once, *i.e.* G1-E and G2-C-E, may be viewed as consequences of effects that occurred on exposed embryos. The observed slow-down in larval growth could be associated with a lower accumulation of storage lipids during the pelagic phase, as remarked with 20% lower lipid index in the first generation larvae issued from exposed embryos; a similar trend was observed in the second generation, although the decrease was not significant. Indeed, bivalve larvae that accumulate less lipids can need more time to reach metamorphosis-competent stage (Talmage and Gobler, 2010) showing the crucial role that lipids play throughout larval development among entry, use and accumulation of stored energy. Lipid storage reduction in response to

embryonic exposure may originate from perturbation in the establishment of larval digestive functions, already suggested by transcriptional profiles in mussel embryos exposed to 50-NH₂ beads (Balbi *et al.*, 2017). Nevertheless, although the extension of time to reach metamorphosis can expose bivalve larvae to more *in situ* stress and mortality (Talmage and Gobler, 2010), the one-day delay observed in the present study for larvae issued from embryonic exposure is low and cannot be extrapolated *in situ* considering the optimal rearing conditions used in our experimental facility. Metamorphosis and settlement success require large amounts of the energy stored during larval development (Bochenek *et al.*, 2001). Here, the settlement yield was similar among treatments, highlighting that suspected effects on the energy accumulation during larval development were not serious enough to impair the larval ability to metamorphose. Therefore, these results suggest negligible repercussions of the embryonic exposure to nano-PS on the oyster larvae. Nevertheless, it should also be considered that the favorable rearing conditions used here may have counteracted any adverse effect. Indeed, harsher environmental conditions during larval growth are expected to emphasize the sensitivity of animals to individual stressors and cocktail effects. To test the occurrence of adverse mid-term effects upon embryonic nano-PS exposure in more realistic conditions, it would be interesting in future works to consider other stressors occurring in natural environment during the larval development (natural food variations/limitations, pathogens, contaminants) in addition to plastic exposures.

Embryonic exposure did not induce phenotype differences at the adult stage. By monitoring the growth, ecophysiology and gametogenesis of the G1 adult oysters over several months, we investigated potential “maladaptive tuning”, *i.e.* emergence of new phenotypes at the adult stage in response to embryonic exposure leading to reduced fitness (Hamdoun and Epel, 2007). For instance, zebrafish exposed to PAH during embryonic development had reduced cardiovascular performances at the adult stage (Hicken *et al.*, 2011). Here, adult oysters displayed similar growth, ecophysiological characteristics and reproductive outputs (gametes and larval quality) whether they had grown from exposed embryos or controls. Therefore, these results imply that the suggested alterations observed at the embryonic and larval stages (cardiolipins relative content, larval growth) upon embryonic exposure to nano-PS at 0.1 µg.mL⁻¹ were compensated as they did not induce any delayed effect in the ecophysiological, growth and reproductive performances of adult oysters in our experimental conditions.

Are there any memory-stress mechanisms occurring upon nano-PS exposure? To understand the risk of contaminants to population stability and estimate population resilience,

it is important to determine how the sensitivity of animals can evolve across generations. Early life stages correspond to an especially sensitive window during which any subtle changes may be transferred across generations owing to the differentiation of primordial germ cells during early development phases. Thus, the environment during early life can induce inter-generational effect in progeny of the next generation (Burton and Melcalfe, 2014). This could occur through epigenetic inheritance, *i.e.* modification of gene expression by adding chemical marks (*e.g.* DNA methylation), that could modify positively or negatively responses to the contaminants over subsequent generations (Vandegheuchte and Janssen, 2014). Although epigenetics research on marine invertebrates is in its infancy, early findings have indicated that DNA methylations are of great importance in the embryonic development success of *C. gigas*. Inhibition of DNA methyltransferase (DNMT) was demonstrated to impact oyster embryolarval development success (Rivière et al., 2013). Moreover, it was recently suggested that modifications of DNA methylation levels of specific homeobox genes can be one of the origins of copper embryotoxicity in oyster (Sussarellu et al., 2018) probably through the negative relationship of transcription level and specific DNA methylation of these homeobox genes (Rivière et al., 2013). In the present study, results did not suggest evidence of epigenetic changes or occurrence of stress-memory mechanism as intergenerational effects were not recorded on the phenotype of G2-larvae issued from embryonic exposure at G1 or both generations. Nevertheless, the first evidence of epigenetic changes in oyster embryos faced to stressors (*i.e.* copper, Sussarellu et al., 2018) and our observation of intermediate but non-significant growth rate of oyster larvae originated from embryos exposed at both generations call for more research to explore adaptive mechanisms during repeated exposure to pollutants such as plastics.

5) Conclusion

Understanding the risks of plastic debris for marine ecosystems implied the assessment of direct effects and potential repercussions after pulsed or chronic exposures. The present study aimed to assess repercussions of embryonic exposure, a sensitive stage which could affect subsequent stages (larvae, juveniles, adults) and generations. Overall, the results suggested that short-term embryonic exposures to amino-nanopolystyrene at $0.1 \mu\text{g.mL}^{-1}$ cause low effects on oyster larvae with a slight but significant growth reduction with no consequences on the settlement yield nor on the adult stage in terms of growth, reproduction and ecophysiological performances. No intergenerational effects were revealed on larvae, the stage we monitored in the second generation. These experimental approaches used under aquaculture procedures

cannot be extrapolated to environmental situations where biological and anthropogenic compounds complexities occur but provide essential data on mechanistic understanding of plastic particles toxicity.

Acknowledgements

This study was supported by the ANR-Nanoplastics project (ANR-15-CE34-0006). K. Tallec has a French doctoral grant from the *Region Bretagne* (50%) and Ifremer (50%). The authors thank the staff of the Ifremer experimental station at Argenton and nursery at Bouin for their help. We thank H McCombie for her help in editing the English.

Disclosure Statement

The authors report no conflict of interest.

References

- Al-Sid-Cheikh, M., Rowland, S.J., Stevenson, K., Rouleau, C., Henry, T.B., and Thompson, R.C., 2018. Uptake, Whole-Body Distribution, and Depuration of Nanoplastics by the Scallop *Pecten maximus* at Environmentally Realistic Concentrations. *Environmental Science & Technology*, 52 (24), 14480–14486.
- Alliegro, M.C. and Wright, D.A., 1983. Polyspermy inhibition in the oyster, *Crassostrea virginica*. *Journal of Experimental Zoology*, 227 (1), 127–137.
- Auguste, M., Balbi, T., Ciacci, C., Canonico, B., Papa, S., Borello, A., Vezzulli, L., and Canesi, L., 2020. Shift in Immune Parameters After Repeated Exposure to Nanoplastics in the Marine Bivalve *Mytilus*. *Frontiers in Immunology*, 11.
- Balbi, T., Camisassi, G., Montagna, M., Fabbri, R., Franzellitti, S., Carbone, C., Dawson, K., and Canesi, L., 2017. Impact of cationic polystyrene nanoparticles (PS-NH₂) on early embryo development of *Mytilus galloprovincialis*: Effects on shell formation. *Chemosphere*, 186, 1–9.
- Bayne, B., 2017. *Biology of Oysters*. Academic P.
- Bayne, B.L., Hawkins, A.J.S., and Navarro, E., 1987. Feeding and digestion by the mussel *Mytilus edulis* L. (Bivalvia: Mollusca) in mixtures of silt and algal cells at low concentrations. *Journal of Experimental Marine Biology and Ecology*, 111 (1), 1–22.

- Beiras, R., Bellas, J., Cachot, J., Cormier, B., Cousin, X., Engwall, M., Gambardella, C., Garaventa, F., Keiter, S., Le Bihanic, F., López-Ibáñez, S., Piazza, V., Rial, D., Tato, T., and Vidal-Liñán, L., 2018. Ingestion and contact with polyethylene microplastics does not cause acute toxicity on marine zooplankton. *Journal of Hazardous Materials*, 360 (July), 452–460.
- Besseling, E., Wang, B., Lürling, M., and Koelmans, A.A., 2014. Nanoplastic affects growth of *S. obliquus* and reproduction of *D. magna*. *Environmental Science & Technology*, 48 (20), 12336–12343.
- Bhandari, R.K., vom Saal, F.S., and Tillitt, D.E., 2015. Transgenerational effects from early developmental exposures to bisphenol A or 17 α -ethinylestradiol in medaka, *Oryzias latipes*. *Scientific Reports*, 5 (1), 9303.
- Bochenek, E., Klinck, J., Powell, E., and Hofmann, E., 2001. A biochemically based model of the growth and development of *Crassostrea gigas* larvae. *Journal of Shellfish Research*, 20 (1), 243–265.
- Boulais, M., Soudant, P., Le Goïc, N., Quéré, C., Boudry, P., and Suquet, M., 2015. Involvement of Mitochondrial Activity and OXPHOS in ATP Synthesis During the Motility Phase of Spermatozoa in the Pacific Oyster, *Crassostrea gigas*. *Biology of Reproduction*, 93 (5), 1–7.
- Burton, T. and Metcalfe, N.B., 2014. Can environmental conditions experienced in early life influence future generations? *Proceedings of the Royal Society B: Biological Sciences*, 281 (1785).
- Chen, Q., Gundlach, M., Yang, S., Jiang, J., Velki, M., Yin, D., and Hollert, H., 2017. Quantitative investigation of the mechanisms of microplastics and nanoplastics toward zebrafish larvae locomotor activity. *Science of The Total Environment*, 584–585, 1022–1031.
- Cole, M., Lindeque, P., Halsband, C., and Galloway, T.S., 2011. Microplastics as contaminants in the marine environment : A review. *Marine Pollution Bulletin*, 62 (12), 2588–2597.
- Conover, R.J., 1966. Assimilation of organic matter by zooplankton. *Limnology and Oceanography*, 11 (3), 338–345.
- Da Costa, F., Petton, B., Mingant, C., Bougaran, G., Rouxel, C., Quéré, C., Wikfors, G.H., Soudant, P., and Robert, R., 2016. Influence of one selected *Tisochrysis lutea* strain rich in

lipids on *Crassostrea gigas* larval development and biochemical composition. *Aquaculture Nutrition*, 22 (4), 813–836.

Dawson, A.L., Kawaguchi, S., King, C.K., Townsend, K.A., King, R., Huston, W.M., and Bengtson Nash, S.M., 2018. Turning microplastics into nanoplastics through digestive fragmentation by Antarctic krill. *Nature Communications*, 9 (1), 1001.

Della Torre, C., Bergami, E., Salvati, A., Faleri, C., Cirino, P., Dawson, K.A., and Corsi, I., 2014. Accumulation and Embryotoxicity of Polystyrene Nanoparticles at Early Stage of Development of Sea Urchin Embryos *Paracentrotus lividus*. *Environmental Science & Technology*, 48 (20), 12302–12311.

Ekvall, M.T., Lundqvist, M., Kelpsiene, E., Šileikis, E., Gunnarsson, S.B., and Cedervall, T., 2019. Nanoplastics formed during the mechanical breakdown of daily-use polystyrene products. *Nanoscale Advances*, 1 (3), 1055–1061.

Eriksen, M., Lebreton, L.C.M., Carson, H.S., Thiel, M., Moore, C.J., Borerro, J.C., Galgani, F., Ryan, P.G., and Reisser, J., 2014. Plastic Pollution in the World's Oceans: More than 5 Trillion Plastic Pieces Weighing over 250,000 Tons Afloat at Sea. *PLoS ONE*, 9 (12), 1–15.

Fabioux, C., Huvet, A., Le Souchu, P., Le Pennec, M., and Pouvreau, S., 2005. Temperature and photoperiod drive *Crassostrea gigas* reproductive internal clock. *Aquaculture*, 250 (1–2), 458–470.

Feng, L., Li, J.-W., Xu, E.G., Sun, X.-D., Zhu, F.-P., Ding, Z.-J., Tian, H.-Y., Dong, S.-S., Xia, P.-F., and Yuan, X.-Z., 2019. Short-term exposure to positively charged polystyrene nanoparticles causes oxidative stress and membrane destruction in cyanobacteria. *Environmental Science: Nano*, 6(10), 3072-3079.

Fitzpatrick, J.L., Nadella, S., Bucking, C., Balshine, S., and Wood, C.M., 2008. The relative sensitivity of sperm, eggs and embryos to copper in the blue mussel (*Mytilus trossulus*). *Comparative Biochemistry and Physiology Part C: Toxicology & Pharmacology*, 147 (4), 441–449.

Foulon, V., Le Roux, F., Lambert, C., Huvet, A., Soudant, P., and Paul-Pont, I. (2016). Colonization of polystyrene microparticles by *Vibrio crassostreae*: light and electron microscopic investigation. *Environmental Science & Technology*, 50(20), 10988-10996.

- Galloway, T.S., Cole, M., and Lewis, C., 2017. Interactions of microplastic debris throughout the marine ecosystem. *Nature Ecology & Evolution*, 1 (5), 0116.
- Geyer, R., Jambeck, J.R., and Law, K.L., 2017. Production, use, and fate of all plastics ever made. *Science Advances*, 3 (7), e1700782.
- Gigault, J., Pedrono, B., Maxit, B., and Ter Halle, A., 2016. Marine plastic litter: the unanalyzed nano-fraction. *Environmental Science: Nano*, 3 (2), 346–350.
- González-Fernández, C., Le Grand, F., Bideau, A., Huvet, A., Paul-Pont, I., and Soudant, P., 2020. Nanoplastics exposure modulate lipid and pigment compositions in diatoms. *Environmental Pollution*, 262, 114274.
- Halpern, B.S., Walbridge, S., Selkoe, K.A., Kappel, C. V., Micheli, F., D'Agrosa, C., Bruno, J.F., Casey, K.S., Ebert, C., Fox, H.E., Fujita, R., Heinemann, D., Lenihan, H.S., Madin, E.M.P., Perry, M.T., Selig, E.R., Spalding, M., Steneck, R., and Watson, R., 2008. A global map of human impact on marine ecosystems. *Science*, 319 (5865), 948–952.
- Hamdoun, A. and Epel, D., 2007. Embryo stability and vulnerability in an always changing world. *Proceedings of the National Academy of Sciences*, 104 (6), 1745–1750.
- Hernandez, L.M., Yousefi, N., and Tufenkji, N., 2017. Are There Nanoplastics in Your Personal Care Products? *Environmental Science & Technology Letters*, 4 (7), 280–285.
- Hicken, C.E., Linbo, T.L., Baldwin, D.H., Willis, M.L., Myers, M.S., Holland, L., Larsen, M., Stekoll, M.S., Rice, S.D., Collier, T.K., Scholz, N.L., and Incardona, J.P., 2011. Sublethal exposure to crude oil during embryonic development alters cardiac morphology and reduces aerobic capacity in adult fish. *Proceedings of the National Academy of Sciences*, 108 (17), 7086–7090.
- His, E. and Maurer, D., 1988. Shell growth and gross biochemical composition of oyster larvae (*Crassostrea gigas*) in the field. *Aquaculture*, 69 (1), 185–194.
- Houtkooper, R.H. and Vaz, F.M., 2008. Cardiolipin, the heart of mitochondrial metabolism. *Cellular and Molecular Life Sciences*, 65 (16), 2493–2506.
- Jaeckle, W.B. and Manahan, D.T., 1989. Growth and Energy Imbalance During the Development of a Lecithotrophic Molluscan Larva (*Haliotis rufescens*). *The Biological Bulletin*, 177 (2), 237–246.

- Jeong, C.B., Won, E.J., Kang, H.M., Lee, M.C., Hwang, D.S., Hwang, U.K., Zhou, B., Souissi, S., Lee, S.J., and Lee, J.S., 2016. Microplastic Size-Dependent Toxicity, Oxidative Stress Induction, and p-JNK and p-p38 Activation in the Monogonont Rotifer (*Brachionus koreanus*). *Environmental Science & Technology*, 50 (16), 8849–8857.
- Julienne, C. M., Tardieu, M., Chevalier, S., Pinault, M., Bougnoux, P., Labarthe, F., & Dumas, J. F. (2014). Cardiolipin content is involved in liver mitochondrial energy wasting associated with cancer-induced cachexia without the involvement of adenine nucleotide translocase. *Biochimica et Biophysica Acta - Molecular Basis of Disease*, 1842(5), 726-733.
- Lambert, S. and Wagner, M., 2016. Formation of microscopic particles during the degradation of different polymers. *Chemosphere*, 161, 510–517.
- Leclère, L., Jager, M., Barreau, C., Chang, P., Le Guyader, H., Manuel, M., and Houliston, E., 2012. Maternally localized germ plasm mRNAs and germ cell/stem cell formation in the cnidarian *Clytia*. *Developmental Biology*, 364 (2), 236–248.
- Lehner, R., Weder, C., Petri-Fink, A., and Rothen-Rutishauser, B., 2019. Emergence of Nanoplastic in the Environment and Possible Impact on Human Health. *Environmental Science & Technology*, 53 (4), 1748–1765.
- Le Grand, F., Soudant, P., Siah, A., Tremblay, R., Marty, Y., and Kraffe, E., 2014. Disseminated neoplasia in the soft-shell clam *Mya arenaria*: Membrane lipid composition and functional parameters of circulating cells. *Lipids*, 49 (8), 807–818.
- Liu, Z., Cai, M., Wu, D., Yu, P., Jiao, Y., Jiang, Q., and Zhao, Y., 2020. Effects of nanoplastics at predicted environmental concentration on *Daphnia pulex* after exposure through multiple generations. *Environmental Pollution*, 256, 113506.
- Major, K.M., DeCourten, B.M., Li, J., Britton, M., Settles, M.L., Mehinto, A.C., Connon, R.E., and Brander, S.M., 2020. Early Life Exposure to Environmentally Relevant Levels of Endocrine Disruptors Drive Multigenerational and Transgenerational Epigenetic Changes in a Fish Model. *Frontiers in Marine Science*, 7.
- Manfra, L., Rotini, A., Bergami, E., Grassi, G., Faleri, C., and Corsi, I. (2017). Comparative ecotoxicity of polystyrene nanoparticles in natural seawater and reconstituted seawater using the rotifer *Brachionus plicatilis*. *Ecotoxicology and environmental safety*, 145, 557-563.

- Mateos-Cárdenas, A., O'Halloran, J., van Pelt, F.N.A.M., and Jansen, M.A.K., 2020. Rapid fragmentation of microplastics by the freshwater amphipod *Gammarus duebeni* (Lillj.). *Scientific Reports*, 10 (1), 12799.
- Mintenig, S.M., Bäuerlein, P.S., Koelmans, A.A., Dekker, S.C., and Van Wezel, A.P., 2018. Closing the gap between small and smaller: towards a framework to analyse nano- and microplastics in aqueous environmental samples. *Environmental Science: Nano*, 5 (7), 1640–1649.
- Miossec, L., Le Deuff, R.-M., and Gouletquer, P., 2009. Alien species alert: *Crassostrea gigas* (Pacific oyster). *ICES Cooperative Research Report*, 299.
- Mottier, A., Kientz-Bouchart, V., Serpentine, A., Lebel, J.M., Jha, A.N., and Costil, K., 2013. Effects of glyphosate-based herbicides on embryo-larval development and metamorphosis in the Pacific oyster, *Crassostrea gigas*. *Aquatic Toxicology*, 128–129, 67–78.
- Moutel, B., Gonçalves, O., Le Grand, F., Long, M., Soudant, P., Legrand, J., Grizeau, D., and Pruvost, J., 2016. Development of a screening procedure for the characterization of *Botryococcus braunii* strains for biofuel application. *Process Biochemistry*, 51 (11), 1855–1865.
- Paradies, G., Paradies, V., De Benedictis, V., Ruggiero, F.M., and Petrosillo, G., 2014. Functional role of cardiolipin in mitochondrial bioenergetics. *Biochimica et Biophysica Acta - Bioenergetics*, 1837 (4), 408–417.
- Paul-Pont, I., Tallec, K., Gonzalez-Fernandez, C., Lambert, C., Vincent, D., Mazurais, D., Zambonino-Infante, J.-L., Brotons, G., Lagarde, F., Fabioux, C., Soudant, P., and Huvet, A., 2018. Constraints and Priorities for Conducting Experimental Exposures of Marine Organisms to Microplastics. *Frontiers in Marine Science*, 5, 1–22.
- Pechenik, J., 1999. On the advantages and disadvantages of larval stages in benthic marine invertebrate life cycles. *Marine Ecology Progress Series*, 177, 269–297.
- Petton, B., Pernet, F., Robert, R., and Boudry, P., 2013. Temperature influence on pathogen transmission and subsequent mortalities in juvenile pacific oysters *Crassostrea gigas*. *Aquaculture Environment Interactions*, 3 (3), 257–273.

- Pousse, É., Flye-Sainte-Marie, J., Alunno-Bruscia, M., Hégaret, H., and Jean, F., 2018. Sources of paralytic shellfish toxin accumulation variability in the Pacific oyster *Crassostrea gigas*. *Toxicon*, 144, 14–22.
- R Core Team (2016). R: A language and environment for statistical computing. R Foundation for Statistical Computing. Vienna, Austria. URL <https://www.R-project.org/>.
- Rafalski, V.A., Mancini, E., and Brunet, A., 2012. Energy metabolism and energy-sensing pathways in mammalian embryonic and adult stem cell fate. *Journal of Cell Science*, 125 (23), 5597–5608.
- Rico-Villa, B., Woerther, P., Mingant, C., Lepiver, D., Pouvreau, S., Hamon, M., and Robert, R., 2008. A flow-through rearing system for ecophysiological studies of Pacific oyster *Crassostrea gigas* larvae. *Aquaculture*, 282 (1–4), 54–60.
- Rivière, G., Wu, G., Fellous, A., Goux, D., Sourdain, P., and Favrel, P., 2013. DNA Methylation Is Crucial for the Early Development in the Oyster *C. gigas*. *Marine Biotechnology*, 15 (6), 739–753.
- Robert, R., and Gérard, A. (1999). Bivalve hatchery technology: the current situation for the Pacific oyster *Crassostrea gigas* and the scallop *Pecten maximus* in France. *Aquatic Living Resources*, 12(2), 121-130.
- Rossi, G., Barnoud, J., and Monticelli, L., 2014. Polystyrene Nanoparticles Perturb Lipid Membranes. *The Journal of Physical Chemistry Letters*, 5 (1), 241–246.
- Savina, M. and Pouvreau, S., 2004. A comparative ecophysiological study of two infaunal filter-feeding bivalves: *Paphia rhomboïdes* and *Glycymeris glycymeris*. *Aquaculture*, 239 (1–4), 289–306.
- Shaikh, S.R., Sullivan, E.M., Alleman, R.J., Brown, D.A., and Zeczycki, T.N., 2014. Increasing mitochondrial membrane phospholipid content lowers the enzymatic activity of electron transport complexes. *Biochemistry*, 53 (35), 5589–5591.
- Sokolova, I.M., Frederich, M., Bagwe, R., Lannig, G., and Sukhotin, A.A., 2012. Energy homeostasis as an integrative tool for assessing limits of environmental stress tolerance in aquatic invertebrates. *Marine Environmental Research*, 79, 1–15.
- Steele, S. and Mulcahy, M.F., 1999. Gametogenesis of the oyster *Crassostrea gigas* in southern Ireland. *Journal of the Marine Biological Association of the United Kingdom*, 79 (4), 673–686.

- Stephens, B., Azimi, P., El Orch, Z., and Ramos, T., 2013. Ultrafine particle emissions from desktop 3D printers. *Atmospheric Environment*, 79, 334–339.
- Sussarellu, R., Suquet, M., Thomas, Y., Lambert, C., Fabioux, C., Pernet, M.E.J., Le Goïc, N., Quillien, V., Mingant, C., Epelboin, Y., Corporeau, C., Guyomarch, J., Robbens, J., Paul-Pont, I., Soudant, P., and Huvet, A., 2016. Oyster reproduction is affected by exposure to polystyrene microplastics. *Proceedings of the National Academy of Sciences*, 201519019.
- Sussarellu, R., Lebreton, M., Rouxel, J., Akcha, F., and Rivière, G., 2018. Copper induces expression and methylation changes of early development genes in *Crassostrea gigas* embryos. *Aquatic Toxicology*, 196, 70–78.
- Talleg, K., Huvet, A., Di Poi, C., González-Fernández, C., Lambert, C., Petton, B., Le Goïc, N., Berchel, M., Soudant, P., and Paul-Pont, I., 2018. Nanoplastics impaired oyster free living stages, gametes and embryos. *Environmental Pollution*, 242, 1226–1235.
- Talmage, S.C. and Gobler, C.J., 2010. Effects of past, present, and future ocean carbon dioxide concentrations on the growth and survival of larval shellfish. *Proceedings of the National Academy of Sciences*, 107 (40), 17246–17251.
- Ter Halle, A., Jeanneau, L., Martignac, M., Jardé, E., Pedrono, B., Brach, L., and Gigault, J., 2017. Nanoplastic in the North Atlantic Subtropical Gyre. *Environmental Science & Technology*, 51 (23), 13689–13697.
- Trevisan, R., Voy, C., Chen, S., and Di Giulio, R.T., 2019. Nanoplastics Decrease the Toxicity of a Complex PAH Mixture but Impair Mitochondrial Energy Production in Developing Zebrafish. *Environmental Science & Technology*, 53(14), 8405-8415.
- Vandegheuchte, M.B. and Janssen, C.R., 2014. Epigenetics in an ecotoxicological context. *Mutation Research - Genetic Toxicology and Environmental Mutagenesis*, 764–765, 36–45.
- van Sebille, E., Wilcox, C., Lebreton, L., Maximenko, N., Hardesty, B.D., van Franeker, J.A., Eriksen, M., Siegel, D., Galgani, F., and Law, K.L., 2015. A global inventory of small floating plastic debris. *Environmental Research Letters*, 10 (12), 124006.
- Vogeler, S., Bean, T.P., Lyons, B.P., and Galloway, T.S., 2016. Dynamics of nuclear receptor gene expression during Pacific oyster development. *BMC Developmental Biology*, 16 (1), 1–13.

Wagner, S. and Reemtsma, T., 2019. Things we know and don't know about nanoplastic in the environment. *Nature Nanotechnology*, 14 (4), 300–301.

Zhang, H., Kuo, Y.Y., Gerecke, A.C., and Wang, J., 2012. Co-release of hexabromocyclododecane (HBCD) and nano- and microparticles from thermal cutting of polystyrene foams. *Environmental Science & Technology*, 46 (20), 10990–10996.

Zhang, Y., and Goss, G. G. (2020). Potentiation of polycyclic aromatic hydrocarbon uptake in zebrafish embryos by nanoplastics. *Environmental Science: Nano*, 7, 1730–1741.

Zhao, L., Qu, M., Wong, G., and Wang, D., 2017. Transgenerational toxicity of nanopolystyrene particles in the range of $\mu\text{g L}^{-1}$ in the nematode *Caenorhabditis elegans*. *Environmental Science: Nano*, 4 (12), 2356–2366.

Table captions

Table 1. Lipid class composition of G1 D-larvae (24 hpf) originating from control embryos (G1-C) and embryos exposed to 50-nm amino-polystyrene beads at $0.1 \mu\text{g.mL}^{-1}$ (G1-E). Lipid classes are expressed as the mass percentage of each class relative to the total lipid content ($n = 12$; mean \pm SE). Comparisons were made using Student's method; **: $p < 0.01$.

Table 2. Distribution of sex and gametogenic stages of G1-C (issued from control embryos) and G1-E (issued from embryos exposed to 50-nm amino-polystyrene beads at $0.1 \mu\text{g.mL}^{-1}$) oysters after 10 weeks of conditioning. Results are expressed as percentages ($n = 20$ oysters per treatment). According to Steele and Mulcahy (1999), gametogenic stages correspond to: (1) developing early active; (2) developing late active; (3) mature.

Figure captions

Figure 1. Experimental design of the embryonic exposures over two generations of oysters. Lightning bolts indicate the 24-h embryonic exposures to 50-nm amino-nanopolystyrene beads (50-NH₂) at $0.1 \mu\text{g.mL}^{-1}$. Parameters analysed at each step are listed on the left-hand side of the figure. Illustrations of the oyster life cycle were adapted from Vogeler *et al.* (2016).

Figure 2. Scanning electron microscopy panel of G1 D-larvae (24 hpf) issued from (A) control embryos (G1-C) or (B and C) embryos exposed to 50-nm amino-polystyrene beads at $0.1 \mu\text{g.mL}^{-1}$ (G1-E). White arrows indicate asperities and holes on the surfaces of the D-larvae. Size in μm is indicated by the scale bar.

Figure 3. Size (μm ; A), lipid index (A.U.; B) and settlement yield (%; C) of G1 larvae issued from control embryos (G1-C; grey) and from embryos exposed to 50 nm amino-polystyrene beads at $0.1 \mu\text{g.mL}^{-1}$ (G1-E; blue). Results are expressed as means \pm SE ($n = 12$). Repeated measures ANOVA were conducted to compare treatments for the size while Student's method was used for the lipid index and the settlement yield at the 5% level; homogeneous groups are indicated by the same letter.

Figure 4. Dry mass (g.oyster^{-1}) of G1-C (grey; issued from control embryos) and G1-E oysters (blue; issued from embryos exposed to 50-nm amino-polystyrene beads at $0.1 \mu\text{g.mL}^{-1}$) during the nursery phase (solid lines; November 2018 – March 2019) and the G1 conditioning period (dashed lines; April 2019 – June 2019). Results are expressed as mean \pm SE ($n = 30$ oysters per sampling date in the nursery monitoring (in common tank) and four replicates (corresponding to four tanks) of 20 oysters per sampling date during the adult experiment). Repeated measures ANOVA were conducted to compare treatments at the 5% level.

Figure 5. Individual clearance rate (A; $\text{L.h}^{-1}.\text{g}^{-1}$ dw std), respiration rate (B; $\text{mg O}_2.\text{h}^{-1}.\text{g}^{-1}$ dw std) and absorption efficiency (%) in adult oysters of G1-C (grey; issued from control embryos) and G1-E (blue; issued from embryos exposed to 50-nm amino-polystyrene beads at $0.1 \mu\text{g.mL}^{-1}$) treatments. Results are expressed as mean \pm SE ($n = 16$ oysters per treatment). Detailed data of the clearance and respiration rates are given in the Supplementary Figure 1. Repeated measures ANOVA were conducted to compare treatments for the clearance and respiration rates while Student's method was used for the absorption efficiency at the 5% level; homogeneous groups are indicated by the same letter.

Figure 6. Size (μm ; A), lipid index (A.U.; B) and settlement yield (%; C) of G2 larvae issued from (i) G1 and G2 control embryos (G2-C-C; grey), (ii) G1 control embryos and G2 embryos exposed to 50-NH₂ at $0.1 \mu\text{g.mL}^{-1}$ (G2-C-E; dashed grey), (iii) G1 embryos exposed to 50-NH₂ at $0.1 \mu\text{g.mL}^{-1}$ and G2 control embryos (G2-E-C; blue), (iv) G1 and G2 embryos exposed to 50-NH₂ at $0.1 \mu\text{g.mL}^{-1}$ (G2-E-E; dashed blue). Results are expressed as means \pm SE ($n = 4$ for size and lipid index; $n = 2$ for the settlement yield). Repeated measures ANOVA were conducted to compare treatments for the size while one-way ANOVA was used for the lipid index at the 5% level; homogeneous groups are indicated by the same letter.

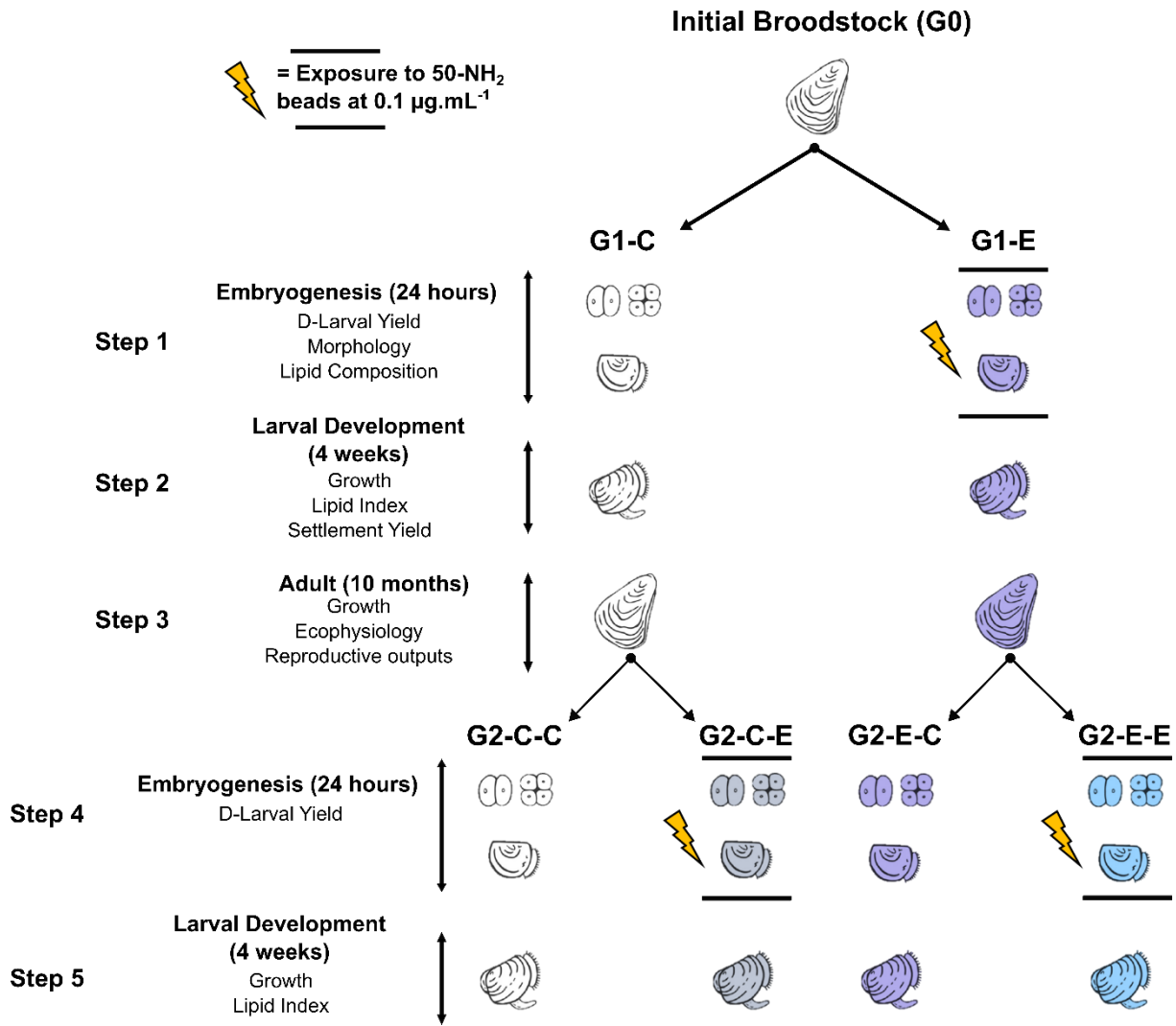


Figure 1.

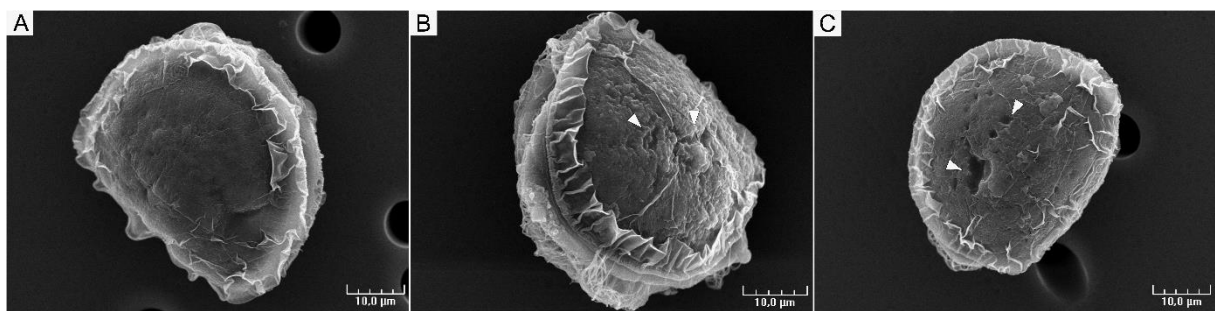


Figure 2.

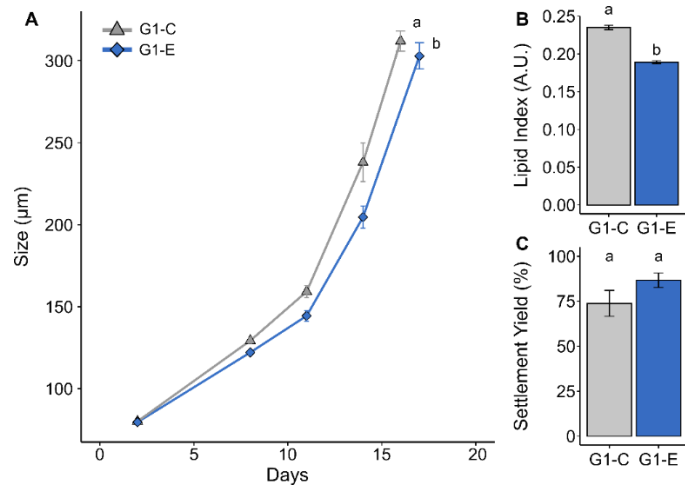


Figure 3.

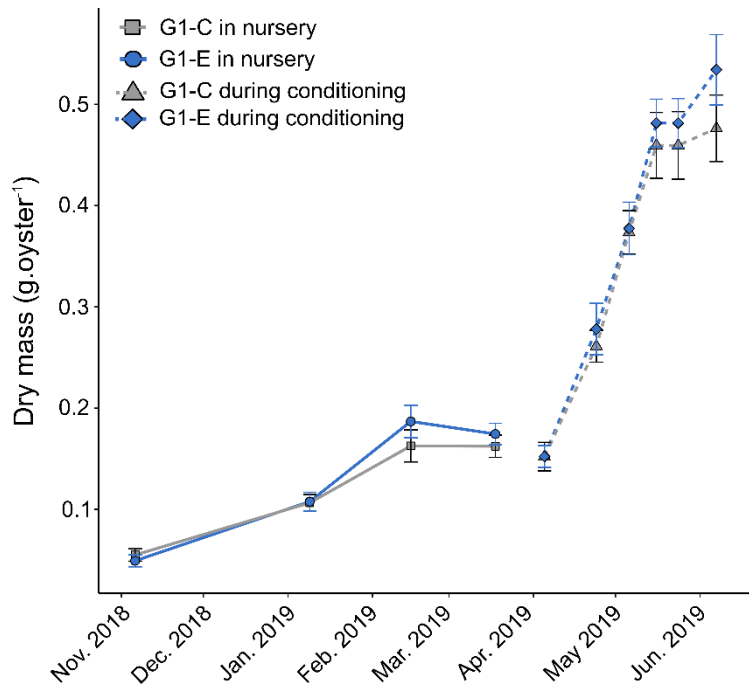


Figure 4.

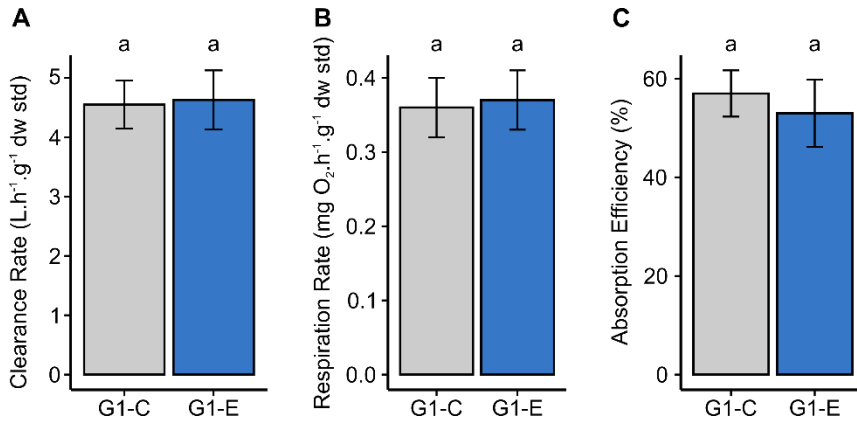


Figure 5.

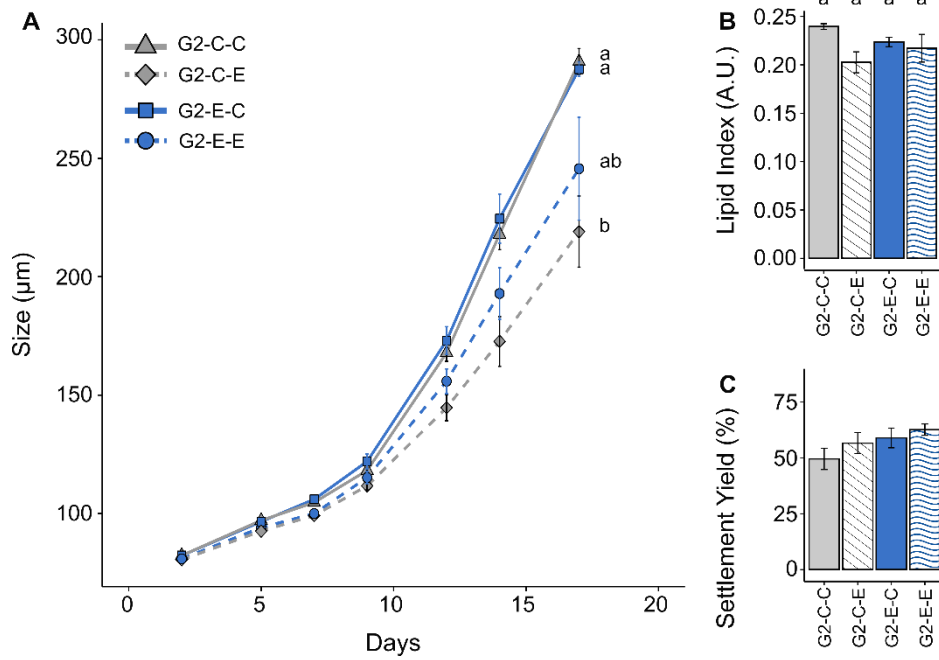


Figure 6.

Table 1.

	Treatments	
	G1-C	G1-E
% TG	50.9 ± 0.6	50.4 ± 0.7
% FFA	0.6 ± 0.1	0.9 ± 0.1
% GE	1.1 ± 0.0	1.1 ± 0.0
% StE	2.8 ± 0.1	3.0 ± 0.2
% Σ Storage lipids	55.4 ± 0.5	55.3 ± 0.7
% ST	3.3 ± 0.1	3.2 ± 0.1
% PC	17.7 ± 0.3	17.4 ± 0.5
% PE	10.2 ± 0.2	10.4 ± 0.2
% PI+CAEP	8.4 ± 0.1	8.2 ± 0.1
% PSer	1.74 ± 0.1	1.67 ± 0.1
% CL	2.51 ± 0.0	2.75 ± 0.1**
% Σ Membrane lipids	44.7 ± 0.5	44.7 ± 0.7
Total lipid content (ng.D-larva ⁻¹)	9.2 ± 0.1	9.5 ± 0.3

TG: triglycerides; StE: sterol esters; GE: glyceryl ethers; FFA: free fatty acids; PE: phosphatidylethanolamine, PI: phosphatidylinositol, PSer: phosphatidylserine, CL: cardiolipin; CAEP: ceramide amino-ethylphosphonate, PC: phosphatidylcholine; ST: sterols.

Table 2.

Treatment	N	Sex (%)			Gametogenic stage (%)		
		Female	Male	Hermaphrodite	1	2	3
G1-C	20	55	40	5	0	15	85
G1-E	20	50	50	0	0	5	95

Supplementary information for

Amino-nanopolystyrene exposures of oyster (*Crassostrea gigas*) embryos affect larval stage over two generations

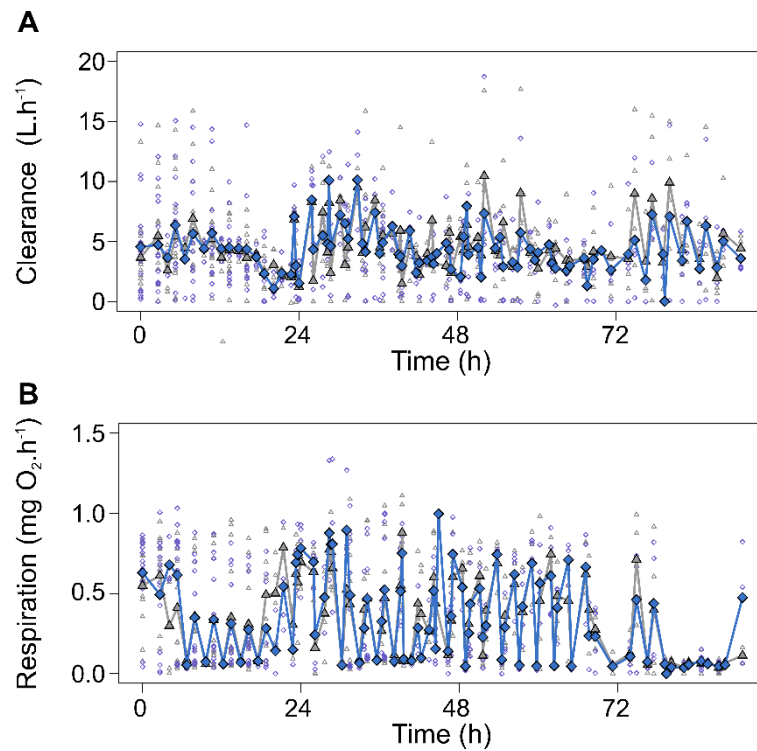
K. Tallec^{1*}, I. Paul-Pont¹, B. Petton¹, M. Alunno-Bruscia¹, C. Bourdon¹, I. Bernardini^{2,3}, M. Boulais¹, C. Lambert¹, C. Quéré¹, A. Bideau¹, N. Le Goïc¹, A-L. Cassone¹, F. Le Grand¹, C. Fabioux¹, P. Soudant¹, A. Huvet^{1*}

¹Univ Brest, Ifremer, CNRS, IRD, LEMAR, F-29280, Plouzané, France.

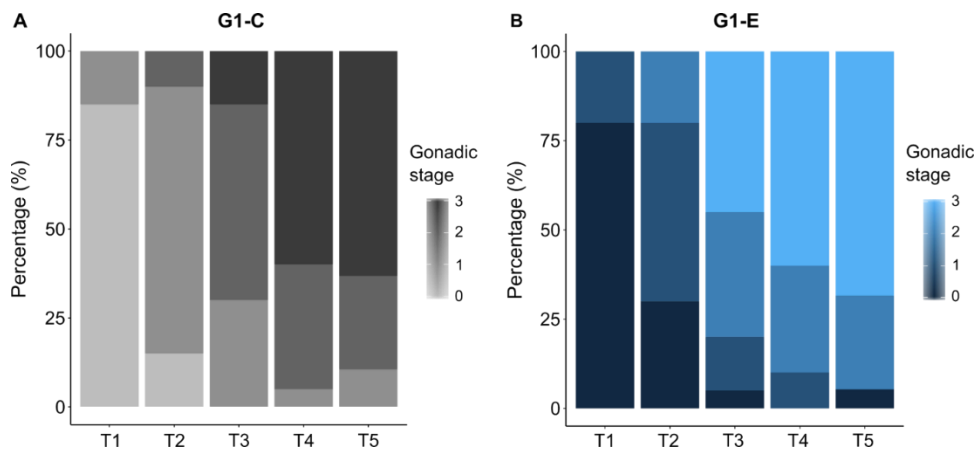
²Dipartimento di Biomedicina Comparata e Alimentazione, Università degli Studi di Padova, Padova, Italy.

³Department of Physical, Earth and Environmental Sciences, University of Siena, Via Mattioli 4, 53100 Siena, Italy.

* kevintallec2@gmail.com; arnaud.huvet@ifremer.fr



Supplementary Figure 1. Standardized clearance (A) and respiration (B) rates of G1-C (grey; issued from control embryos) and G1-E adult oysters (blue; issued from exposed embryos to 50-nm amino-polystyrene beads at $0.1 \mu g \cdot mL^{-1}$) over the 4 trials ($n = 16$ oysters per condition). Empty symbols correspond to all individual measurements; filled symbols correspond to the mean values of each acquisition cycle.



Supplementary Figure 2. Distribution of gametogenic stages at 0 (T1), 2 (T2), 4 (T3), 6 (T4) and 8 (T5) weeks of conditioning in G1-C oysters (A) and G1-E oysters (B). For each date, 20 oysters per condition were sampled per treatment.

Supplementary Table 1. Polar fatty acids of oyster D-larvae issued from control embryos (G1-C) or exposed embryos to 50 nm amino-polystyrene beads at 0.1 $\mu\text{g}\cdot\text{mL}^{-1}$ (G1-E). FAs are expressed as the mass percentage of each FA in the total polar FA content (n = 12; mean \pm SE). Comparisons were made between treatments using a one-way analysis of similarities (ANOSIM) at the 5% level.

	Treatment	
	G1-C	G1-E
iso17:0	0.33 \pm 0.01	0.32 \pm 0.01
ant17:0	0.36 \pm 0.01	0.35 \pm 0.01
Σ BRANCHED	0.69 \pm 0.01	0.67 \pm 0.01
14:0	1.07 \pm 0.04	1.10 \pm 0.04
15:0	0.27 \pm 0.01	0.26 \pm 0.01
16:0	16.49 \pm 0.23	16.36 \pm 0.21
17:0	0.87 \pm 0.01	0.86 \pm 0.02
18:0	5.10 \pm 0.09	4.84 \pm 0.07
Σ SFA	23.79 \pm 0.29	23.42 \pm 0.27
16:1n-9	0.24 \pm 0.04	0.28 \pm 0.02
16:1n-7	1.08 \pm 0.06	1.12 \pm 0.05
18:1n-9	1.49 \pm 0.02	1.54 \pm 0.02
18:1n-7	2.57 \pm 0.07	2.62 \pm 0.07
18:1n-5	0.32 \pm 0.03	0.31 \pm 0.02
20:1n-11	1.90 \pm 0.03	1.80 \pm 0.03
20:1n-9	0.44 \pm 0.02	0.43 \pm 0.01
20:1n-7	3.61 \pm 0.04	3.54 \pm 0.04
22:1n-11	0.93 \pm 0.03	0.89 \pm 0.02
22:1n-9	5.11 \pm 0.06	4.79 \pm 0.07
Σ MUFA	17.67 \pm 0.11	17.32 \pm 0.13
18:2n-6	0.84 \pm 0.01	0.88 \pm 0.02
18:3n-3	1.11 \pm 0.03	1.19 \pm 0.02
18:4n-3	1.76 \pm 0.04	1.84 \pm 0.03
20:4n-6	1.80 \pm 0.04	1.72 \pm 0.02
20:5n-3	19.93 \pm 0.16	20.84 \pm 0.17
21:5n-3	0.83 \pm 0.01	0.85 \pm 0.01
22:5n-6	0.79 \pm 0.03	0.80 \pm 0.02
22:5n-3	1.88 \pm 0.04	1.95 \pm 0.04
22:6n-3	15.59 \pm 0.32	15.40 \pm 0.32
20:2j	0.63 \pm 0.02	0.56 \pm 0.05
Σ PUFA	45.16 \pm 0.29	46.03 \pm 0.36
16:1n-7DMA	1.52 \pm 0.04	1.62 \pm 0.06
18:0DMA	7.31 \pm 0.12	7.18 \pm 0.23
Σ DMA	8.83 \pm 0.10	8.80 \pm 0.21
Σ Unknown (3 FA)	0.93 \pm 0.03	0.98 \pm 0.04

Supplementary Table 2. Neutral fatty acids of oyster D-larvae issued from control embryos (G1-C) or embryos exposed to 50-nm amino-polystyrene beads at 0.1 $\mu\text{g}\cdot\text{mL}^{-1}$ (G1-E). FAs are expressed as the mass percentage of each FA in the total neutral FA content (n = 12; mean \pm SE). Comparisons were made between treatments using a one-way analysis of similarities (ANOSIM) at the 5% level.

	Treatment	
	G1-C	G1-E
iso17:0	0.41 \pm 0.00	0.42 \pm 0.01
Σ BRANCHED	1.03 \pm 0.01	1.08 \pm 0.03
14:0	5.72 \pm 0.16	5.92 \pm 0.18
15:0	0.44 \pm 0.00	0.47 \pm 0.02
16:0	25.61 \pm 0.10	26.70 \pm 0.94
17:0	0.86 \pm 0.01	0.90 \pm 0.03
18:0	4.05 \pm 0.06	4.41 \pm 0.18
Σ SFA	36.82 \pm 0.25	38.58 \pm 1.24
16:1n-9	0.30 \pm 0.00	0.29 \pm 0.03
16:1n-7	5.83 \pm 0.35	5.78 \pm 0.33
16:1n-5	0.30 \pm 0.00	0.30 \pm 0.01
18:1n-11	0.26 \pm 0.01	0.25 \pm 0.01
18:1n-9	3.77 \pm 0.02	3.65 \pm 0.12
18:1n-7	5.02 \pm 0.11	4.92 \pm 0.09
18:1n-5	0.24 \pm 0.01	0.29 \pm 0.05
20:1n-11	0.93 \pm 0.02	0.90 \pm 0.03
20:1n-9	0.22 \pm 0.01	0.22 \pm 0.01
20:1n-7	2.44 \pm 0.04	2.32 \pm 0.11
Σ MUFA	19.31 \pm 0.45	18.93 \pm 0.36
16:2n-4	0.22 \pm 0.01	0.21 \pm 0.01
16:3n-4	0.29 \pm 0.01	0.30 \pm 0.01
18:2n-6	2.03 \pm 0.02	1.96 \pm 0.07
18:2n-4	0.36 \pm 0.01	0.33 \pm 0.01
18:3n-3	3.14 \pm 0.06	3.02 \pm 0.13
18:4n-3	5.87 \pm 0.07	5.65 \pm 0.19
20:4n-6	0.57 \pm 0.00	0.55 \pm 0.01
20:4n-3	0.79 \pm 0.01	0.76 \pm 0.02
20:5n-3	12.57 \pm 0.11	12.12 \pm 0.34
21:5n-3	1.09 \pm 0.01	1.03 \pm 0.04
22:5n-6	0.32 \pm 0.01	0.32 \pm 0.01
22:5n-3	0.81 \pm 0.02	0.89 \pm 0.06
22:6n-3	8.24 \pm 0.12	7.88 \pm 0.29
20:2j	1.38 \pm 0.03	1.29 \pm 0.06
22:2j	2.85 \pm 0.05	2.71 \pm 0.14
22:2i	0.36 \pm 0.01	0.33 \pm 0.01
Σ PUFA	42.22 \pm 0.32	40.64 \pm 1.01

18:0DMA	0.45 ± 0.01	0.57 ± 0.05
Σ DMA	0.45 ± 0.01	0.57 ± 0.05
Σ Unknown (2 FA)	0.17 ± 0.01	0.20 ± 0.02
Σ Others ^a	2.09 ± 0.01	2.12 ± 0.01

^a Others: iso15:0, ant15:0, iso16:0, ant17:0, 24:0, 16:3n-3, 16:4n-3, 18:3n-6, 18:3n-4, 18:4n-1, 20:2i, 20:2n-6, 20:3n-6, 20:3n-3, each accounting for less than 0.2% of the total FA.

Supplementary Table 3. Survival (%) of G1 and G2 larvae (n = 12 for G1 and 4 for G2; means \pm SE).

	Survival (%)	
	Mean	SE
G1-C	55.6	4.9
G1-E	43.9	4.7
G2-C-C	40.2	9.7
G2-C-E	33.6	6.9
G2-E-C	19.3	9.3
G2-E-E	20.0	9.2